Stochastic Modelling of Wave Loads on Floating Bridges: Efficient Calculation of Cross-Spectral Densities

Finn-Idar Grøtta Giske

Norwegian University of Science and Technology, Trondheim, Norway

Multiconsult, Oslo, Norway

Bernt Johan Leira, Ole Øiseth

Norwegian University of Science and Technology, Trondheim, Norway

Contact: finn.i.giske@ntnu.no

Abstract

This paper outlines a fast and accurate approach for calculation of the auto- and cross-spectral densities in the stochastic modelling of wave loads on floating bridges. For long-term response predictions used in extreme response assessment and fatigue design, the efficiency of this approach may prove valuable. An illustration of the approach is given for a pontoon type floating bridge, and the performance is compared with the traditional computation method. The gain in computational effort is seen to increase with increasing bridge length.

Keywords: Floating bridge; pontoon; wave excitation load; directional waves; cross-spectral density.

1 Introduction

New technologies for crossing wide and deep fjords are currently focused upon in Norway, especially in connection with the Norwegian Public Roads Administration project “Coastal Highway Route E39”. In order to facilitate the design of cost-efficient and reliable fjord crossing structures, the development of robust and fast methods for calculating environmental loads is important. The subject of the present paper is computation of the spectral characteristics for the wave loads acting on pontoon bridges. This is an important input for dynamic analysis of floating bridges both in time and frequency domain [1, 2]. Especially for long-term response predictions, efficiency is vital [3].

This paper outlines new formulations for calculation of the auto- and cross-spectral densities in relation to the stochastic modelling of wave loads. Auto- and cross-spectral densities are generally expressed in terms of an integral that traditionally has been computed using numerical quadrature. For this straightforward approach, the computational effort increases with increasing distance between the pontoons due to rapid oscillation of the relevant analytical functions. The new approach avoids this effect of increasing computational efforts by a reformulation of the basic expressions.

An application of the approach is demonstrated in relation to a pontoon bridge, and the performance is compared with the more traditional method. The gain in computational effort (as compared to the traditional method) is seen to increase when the number of pontoons increases and when the distance between the pontoons increases.

2 Stochastic modelling of waves and wave loads

2.1 Stochastic modelling of waves

A common approach when modelling wind-generated waves for engineering purposes is to assume that the sea elevation is a homogeneous and stationary stochastic process [4]. The sea elevation at the point (x, y) at time t, denoted $\eta(x, y, t)$, is then written as

$$\eta(x,y,t) = \int_{-\infty}^{\infty} e^{i\omega t - i\boldsymbol{\kappa}\cdot[x,y]} dB(\boldsymbol{\kappa}, \omega), \qquad (1)$$

where $\boldsymbol{\kappa} = [\kappa\cos\theta\,, \kappa\sin\theta]$ is the wave number vector, ω is the angular frequency and $B(\boldsymbol{\kappa}, \omega)$ is the spectral process associated with the wave elevation. Assuming linear wave theory, the dispersion relation $\omega^2 = \kappa g \tanh(\kappa d)$ provides a one-to-one mapping between the frequency and the wave number, and we may write the wave number $\kappa(\omega)$ as a function of ω.

Under these assumptions the cross-spectral density between the wave elevation at two points (x_m, y_m) and (x_n, y_n) can be expressed as

$$S_{mn}(\omega) = S_{\eta\eta}(\omega) \int_{-\pi}^{\pi} \Psi(\theta,\omega)\, e^{-i\kappa(\omega)(\Delta x\cos\theta + \Delta y\sin\theta)} d\theta, \qquad (2)$$

where $\Delta x = x_m - x_n$ and $\Delta y = y_m - y_n$. $S_{\eta\eta}(\omega)$ is the one-dimensional spectral density and $\Psi(\theta, \omega)$ is the spreading function. Various theoretical models for $S_{\eta\eta}(\omega)$ and $\Psi(\theta, \omega)$ are available in the literature [5, 6]. The cross-spectral densities are important in engineering applications because they fully describe the second order statistics of the stochastic process.

2.2 Stochastic modelling of wave loads

2.2.1 Wave excitation forces on a pontoon

Consider a pontoon with a local coordinate system $(\tilde{x}, \tilde{y})$, which is located with its origin at the point (x_0, y_0) and rotated counterclockwise with an angle α_0 relative to the global coordinate system (x, y) as shown in Figure 1. Thus (x_0, y_0) and α_0 specifies the location and orientation of the pontoon. With this definition, the global and local coordinates are related by

$$\begin{bmatrix} x \\ y \end{bmatrix} = \begin{bmatrix} x_0 + \tilde{x}\cos\alpha_0 - \tilde{y}\sin\alpha_0 \\ y_0 + \tilde{x}\sin\alpha_0 + \tilde{y}\cos\alpha_0 \end{bmatrix}. \qquad (3)$$

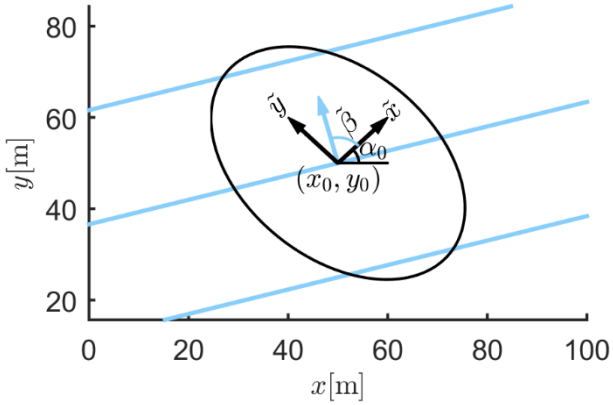

Figure 1. Local coordinate system of a pontoon.

Within the framework of linear potential theory, the hydrodynamic forces acting on a body of arbitrary shape can be computed using a panel method as implemented in software such as WADAM [7]. The wave excitation forces are then reported in terms of the complex transfer function from the wave elevation to the wave load. This means that for a regular incident wave of amplitude A given in local coordinates by

$$\eta(\tilde{x}, \tilde{y}, t) = Ae^{i\omega t - i\kappa(\tilde{x}\cos\tilde{\beta} + \tilde{x}\sin\tilde{\beta})}, \qquad (4)$$

the forces and moments due to this wave can be expressed as $A\boldsymbol{f}_0(\tilde{\beta}, \omega)e^{i\omega t}$, where $\boldsymbol{f}_0(\tilde{\beta}, \omega)$ is the complex transfer function. Here $\tilde{\beta}$ is the wave propagation direction given as the angle relative to the $\tilde{x}$-axis, see Figure 1.

The vector $\boldsymbol{f}_0(\tilde{\beta}, \omega)$ contains six components, the transfer functions for three forces and three moments. Figure 2 shows an example of a transfer function for the force in the sway-direction, i.e. the force along the $\tilde{y}$-axis.

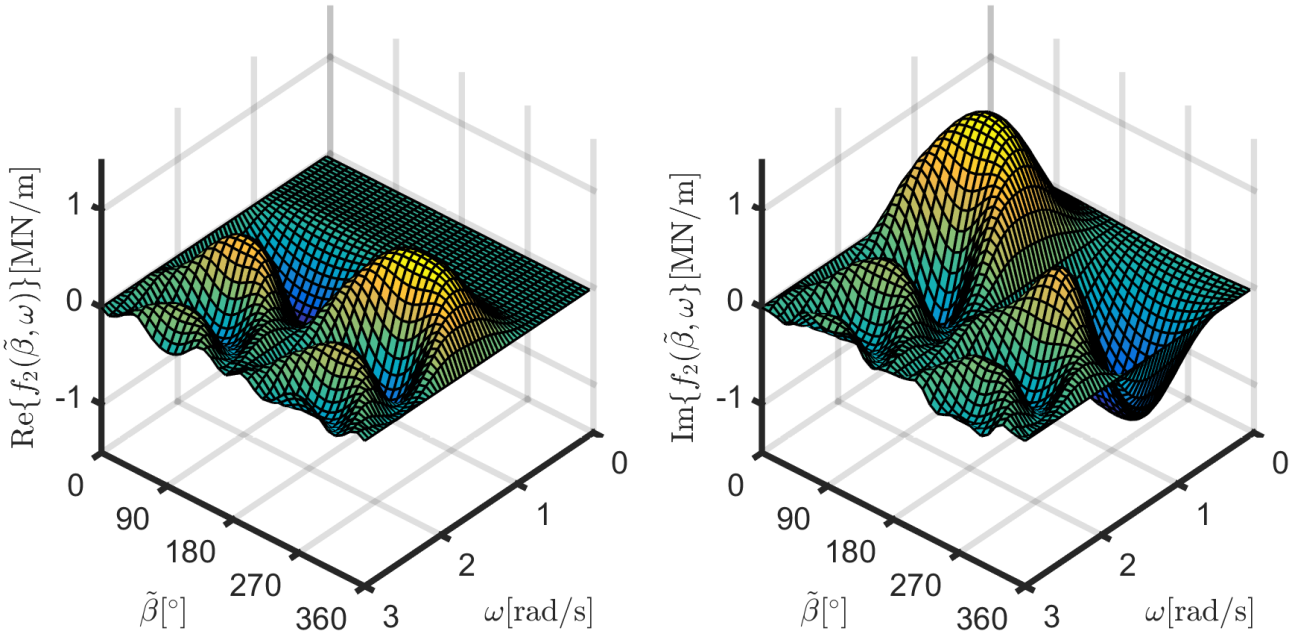

Figure 2. The transfer function for the sway force ($\tilde{y}$-direction) on one pontoon, given by its real part (left) and imaginary part (right).

Because linear wave theory is assumed, the load due to the irregular wave (1) can be found by superposition. Specifically we have that the stochastic wave load is given by

$$\boldsymbol{q}_0(t) = \int_{-\infty}^{\infty} \boldsymbol{f}_0(\theta - \alpha_0, \omega) e^{i\omega t - i\boldsymbol{\kappa}\cdot[x_0, y_0]} dB(\boldsymbol{\kappa}, \omega). \quad (5)$$

2.2.2 Cross-spectral densities

We now consider the wave excitation loads on the Bergsøysund floating bridge located on the north-west coast of Norway. This is a pontoon type floating bridge with seven pontoons. The pontoons are located at points (x_1, y_1), (x_2, y_2), …, (x_7, y_7), with orientation angles α_1, α_2, …, α_7 relative to the global x-axis, as illustrated in Figure 3. We assume that the pontoons are far enough apart so that interaction effects can be neglected.

Now the wave loads acting on each pontoon can be expressed as in (5), and the load vector for the whole bridge is defined by $\boldsymbol{q} = [\boldsymbol{q}_1^T, \boldsymbol{q}_2^T, \dots, \boldsymbol{q}_7^T]^T$. Because each pontoon is loaded in six degrees of freedom (dofs), the total number of dofs for the bridge will be $7 \cdot 6 = 42$. Assigning to each dof an index $\mu \in \{1,2,\dots,42\}$, the individual components of the load vector $\boldsymbol{q}$ can be denoted by q_μ. Using the expression (5) for the loads, the cross-spectral density between the loads q_μ and q_ν is given by

$$\frac{S_{q_\mu q_\nu}(\omega)}{S_{\eta\eta}(\omega)} = \int_{-\pi}^{\pi} \Psi(\theta, \omega) f_\mu(\theta - \alpha_m, \omega) \overline{f_\nu(\theta - \alpha_n, \omega)} e^{-i\kappa(\omega)(\Delta x \cos\theta + \Delta y \sin\theta)} d\theta. \quad (6)$$

The index m is the pontoon number corresponding to the global dof μ, and is given by $m = \lceil \mu/6 \rceil$, where $\lceil \cdot \rceil$ denotes the ceiling function. Similarly $n = \lceil \nu/6 \rceil$.

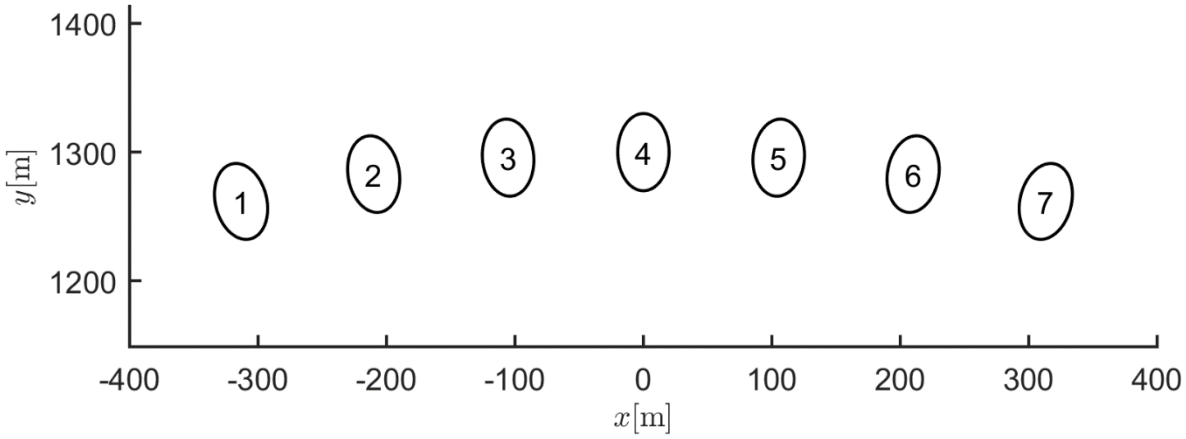

Figure 3. Pontoon locations and orientations for the Bergsøysund floating bridge.

3 Series expansion solution

The integral (6) for the cross-spectral densities has traditionally been calculated using numerical integration. In this paper, however, we pursue an exact solution in terms of a series expansion.

3.1 Solving the integral

If the factor $\Psi(\theta,\omega)f_\mu(\theta-\alpha_m,\omega)\overline{f_\nu(\theta-\alpha_n,\omega)}$ is written as a Fourier series in θ, the integral (6) can be solved in terms of Bessel functions using the approach found in Section 7.2.1 of [8]. If we have that

$$\Psi(\theta,\omega)f_\mu(\theta-\alpha_m,\omega)\overline{f_\nu(\theta-\alpha_n,\omega)} = \sum_{k=-\infty}^{\infty} C_k^{\mu\nu}(\omega)\, e^{ik\theta}, \tag{7}$$

the integral (6) can be expressed as

$$\frac{S_{q_\mu q_\nu}(\omega)}{S_{\eta\eta}(\omega)} = \int_{-\pi}^{\pi}\sum_{k=-\infty}^{\infty} C_k^{\mu\nu}(\omega)\, e^{ik\theta}\, e^{i\kappa(\omega)L\cos(\theta+\beta)}d\theta, \tag{8}$$

where $L=\sqrt{\Delta x^2+\Delta y^2}$, $\beta=\pi-\operatorname{atan2}(\Delta y,\Delta x)$, and $\operatorname{atan2}(\Delta y,\Delta x)$ is the generalization of $\arctan(\Delta y/\Delta x)$ that covers the entire circular range. Using known identities for Bessel functions the integral (8) can finally be solved term-by-term, giving

$$\frac{S_{q_\mu q_\nu}(\omega)}{S_{\eta\eta}(\omega)} = 2\pi\sum_{k=-\infty}^{\infty} C_k^{\mu\nu}(\omega) i^k e^{-ik\beta} J_k(\kappa(\omega)L), \tag{9}$$

where $J_k(\cdot)$ denotes the Bessel function of the first kind with integer order k.

3.2 Obtaining the Fourier coefficients $C_k^{\mu\nu}(\omega)$

The transfer functions $f_\mu(\tilde{\beta},\omega)$ are usually known only by their values at a finite number $N_{\tilde{\beta}}$ of heading angles $\tilde{\beta}$, which we assume are evenly distributed in the interval $[0,2\pi)$. For our purpose, it is convenient to define the transfer functions using trigonometric interpolation, which means that they can be written as

$$f_\mu(\tilde{\beta},\omega) = \sum_{k=-N_f}^{N_f} a_k^\mu(\omega) e^{ik\tilde{\beta}}, \tag{10}$$

where the coefficients $a_k^\mu(\omega)$ can be computed using the fast Fourier transform (FFT), and $N_f = \lfloor N_{\tilde{\beta}}/2 \rfloor$. With transfer functions given by (10) we have that

$$\begin{aligned} f_\mu(\theta-\alpha_m,\omega) &= \sum_{k=-N_f}^{N_f}\left(e^{-ik\alpha_m}a_k^\mu(\omega)\right)e^{ik\theta}, \\ \overline{f_\nu(\theta-\alpha_n,\omega)} &= \sum_{k=-N_f}^{N_f}\left(\overline{e^{ik\alpha_n}a_{-k}^\nu(\omega)}\right)e^{ik\theta}. \end{aligned} \tag{11}$$

It can be shown that the Fourier coefficients of a product are given by the convolution between the Fourier coefficients of the factors. Thus we have

$$f_\mu(\theta-\alpha_m,\omega)\overline{f_\nu(\theta-\alpha_n,\omega)} = \sum_{k=-2N_f}^{2N_f} A_k^{\mu\nu}(\omega)\, e^{ik\theta}, \quad (12)$$

where $A_k^{\mu\nu}(\omega)$ is computed by taking the convolution between the coefficients $\{e^{-ik\alpha_m}a_k^\mu(\omega)\}_{k=-N_f}^{N_f}$ and $\{\overline{e^{ik\alpha_n}a_{-k}^\nu(\omega)}\}_{k=-N_f}^{N_f}$.

Finally, assuming the spreading function is known by its Fourier coefficients as

$$\Psi(\theta,\omega) = \sum_{k=-\infty}^{\infty} c_k(\omega)e^{ik\theta}, \quad (13)$$

the Fourier coefficients $C_k^{\mu\nu}(\omega)$ in (7) are given by the convolution between $\{c_k(\omega)\}_{k=-\infty}^{\infty}$ and $\{A_k^{\mu\nu}(\omega)\}_{k=-2N_f}^{2N_f}$, i.e.

$$C_k^{\mu\nu}(\omega) = \sum_{r=-2N_f}^{2N_f} A_r^{\mu\nu}(\omega)c_{k-r}(\omega). \quad (14)$$

3.3 Auto-spectral density and complex coherency

For the cross-spectral densities between loads at the same pontoon we have that $m=n$, which means that $L=0$. For the Bessel functions we have that $J_k(0)=0$ for any integer k, with the exception $J_0(0)=1$. If we use this in the formula (9), we obtain

$$S_{q_\mu q_\nu}(\omega) = 2\pi S_{\eta\eta}(\omega)C_0^{\mu\nu}(\omega), \quad (15)$$

which holds whenever μ and ν are dofs on the same pontoon. This can be expressed as $\lceil \mu/6 \rceil = \lceil \nu/6 \rceil$. In particular, when $\mu=\nu$, (15) gives an expression for the auto-spectral density:

$$S_{q_\mu q_\mu}(\omega) = 2\pi S_{\eta\eta}(\omega)C_0^{\mu\mu}(\omega). \quad (16)$$

Using the formulas (15) and (16) will reduce the computation time, since only the coefficient $C_0^{\mu\nu}(\omega)$ needs to be calculated.

The complex coherency is defined as

$$\gamma_{q_\mu q_\nu}(\omega) = \frac{S_{q_\mu q_\nu}(\omega)}{\sqrt{S_{q_\mu q_\mu}(\omega)}\sqrt{S_{q_\nu q_\nu}(\omega)}}. \quad (17)$$

Inserting (9) and (16), we obtain the formula

$$\gamma_{q_\mu q_\nu}(\omega) = \sum_{k=-\infty}^{\infty} \frac{C_k^{\mu\nu}(\omega)i^k e^{-ik\beta}J_k(\kappa(\omega)L)}{\sqrt{C_0^{\mu\mu}(\omega)C_0^{\nu\nu}(\omega)}}. \quad (18)$$

The complex coherency is dimensionless, it satisfies $\left|\gamma_{q_\mu q_\nu}(\omega)\right| \le 1$ and it will be independent of the one-dimensional spectral density $S_{\eta\eta}(\omega)$. In computations, it is therefore reasonable to first calculate the complex coherencies by (18) and the auto-spectral densities by (16). The cross-spectral densities can then be obtained using (17) as $S_{q_\mu q_\nu}(\omega) = \sqrt{S_{q_\mu q_\mu}(\omega)}\gamma_{q_\mu q_\nu}(\omega)\sqrt{S_{q_\nu q_\nu}(\omega)}$.

4 Model setup

In order to calculate the auto- and cross-spectral densities, specific models for the spreading function $\Psi(\theta,\omega)$ and the one-dimensional spectral density $S_{\eta\eta}(\omega)$ has to be chosen. Ideally, this should be done according to on-site measurements of the environmental conditions, but in this paper the choices are somewhat arbitrary since the purpose is to illustrate the computational method.

4.1 Spreading function

The most commonly used spreading function, and the one that is used here, is the *cos-2s* type spreading function. This is given by

$$\Psi(\theta,\omega) = \frac{2^{2s}\Gamma^2(s+1)}{2\pi\Gamma(2s+1)}\left(\cos^2\frac{\theta-\bar{\theta}}{2}\right)^s, \quad (19)$$

where $\bar{\theta}$ is the mean wave direction (relative to the global x-axis) and s is the (possibly ω-dependent) spreading parameter that determines the crest length of the waves. Figure 4 shows the spreading function for different values of s. Small values of s give significant wave contributions in almost all directions, resulting in short crested waves,

whereas large values of s give contributions mainly in the mean wave direction, resulting in long crested waves.

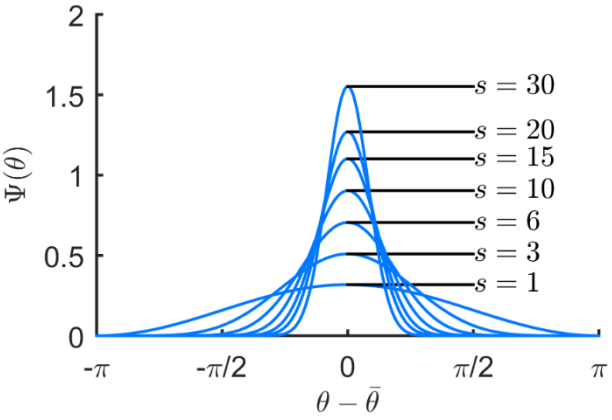

Figure 4. The cos-2s spreading function for different values of s.

For the calculation of the Fourier coefficients $C_k^{\mu\nu}(\omega)$, the spreading function should be given by its Fourier coefficients as in (13). It can be shown that for the *cos-2s* spreading function the Fourier coefficients are given by

$$c_k(\omega) = \frac{e^{-ik\bar{\theta}}\Gamma^2(s+1)}{2\pi\Gamma(s-k+1)\Gamma(s+k+1)}, \qquad (20)$$

which holds for any positive real value s.

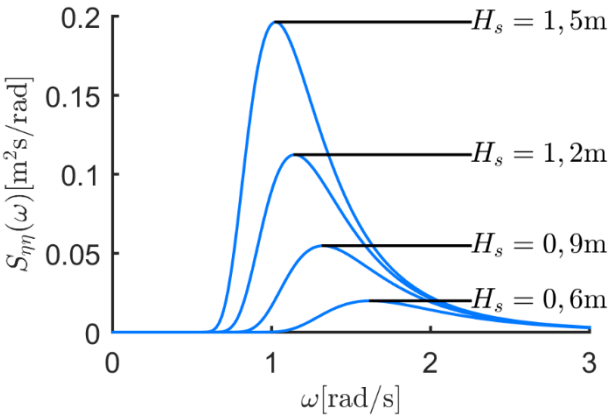

Figure 5. The one-parameter Pierson-Moskowitz spectrum for different values of H_s.

4.2 One-dimensional spectral density

For the one-dimensional wave spectral density the one-parameter Pierson-Moskowitz spectrum [6] is used. The input parameter is the significant wave height $H_s = 4\sigma_\eta$, where σ_η is the standard deviation of the wave elevation. Thus, the value H_s determines the severity of the sea state. Figure 5 shows the wave spectrum for some values of H_s.

5 Results

All auto- and cross-spectral densities for the wave excitation load of the Bergsøysund floating bridge were calculated using the method described in Section 3. The series expansion (18) was used, including enough terms to make the complex coherencies $\gamma_{q_\mu q_\nu}(\omega)$ exact within a tolerance of 10^{-3}.

In applications, it is usually of interest to calculate the cross-spectral densities for a number of different sea states. It is therefore important to notice that the coefficients $A_k^{\mu\nu}(\omega)$ only depend on the structure, and not on the sea state. In addition, the complex coherency $\gamma_{q_\mu q_\nu}(\omega)$ is independent of the one-dimensional spectral density.

5.1 Calculated auto- and cross-spectral densities

We now consider a sea state defined by a spreading $s = 10$, a mean wave direction $\bar{\theta} = \pi/2$ (i.e. transverse to the bridge arch in the horizontal plane) and a significant wave height $H_s = 0{,}9$ m.

The auto-spectral density $S_{q_{20}q_{20}}(\omega)$ for the load in the sway direction ($\tilde{y}$-direction) of pontoon 4 is shown in Figure 6 (left). From the auto-spectral density, the auto-covariance function $C_{q_{20}q_{20}}(\tau) = \mathrm{E}[q_{20}(t+\tau)q_{20}(t)]$ is obtained by taking the Fourier transform. In particular, the variance of the load in this direction is obtained as the value $C_{q_{20}q_{20}}(0)$.

Figure 7 (left) shows the cross-spectral density $S_{q_8q_{20}}(\omega)$ between the loads in the sway directions of pontoon 2 and pontoon 4. In the same way as in Figure 6, the cross-covariance function $C_{q_8q_{20}}(\tau) = \mathrm{E}[q_8(t+\tau)q_{20}(t)]$ is obtained by the Fourier transform. Now the value $C_{q_8q_{20}}(0)$ gives the covariance of the respective loads.

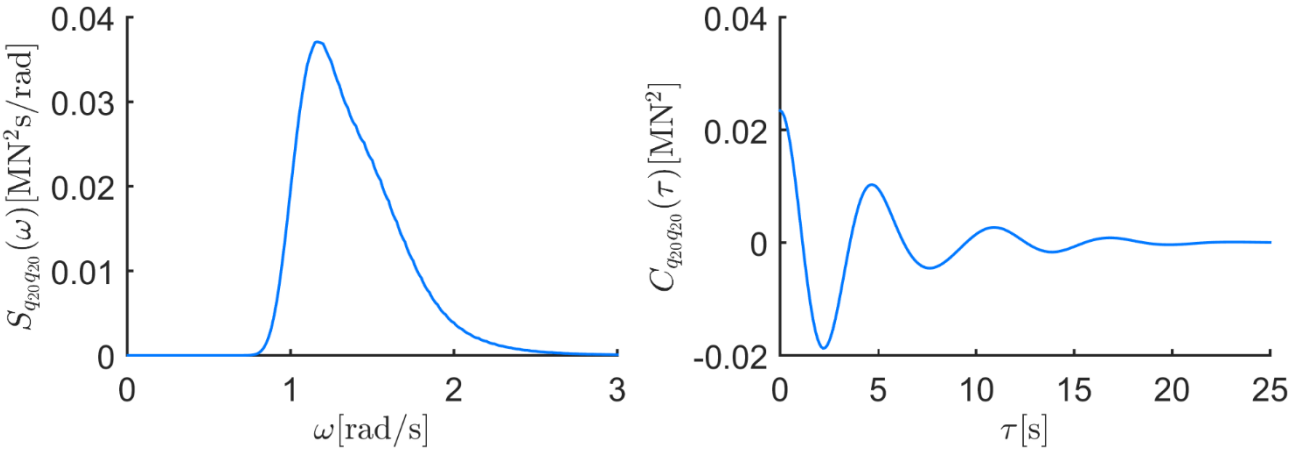

Figure 6. The auto-spectral density $S_{q_{20}q_{20}}(\omega)$ (left) for the load in the sway direction ($\tilde{y}$-direction) of pontoon 4, along with the corresponding auto-covariance function $C_{q_{20}q_{20}}(\tau)$ (right).

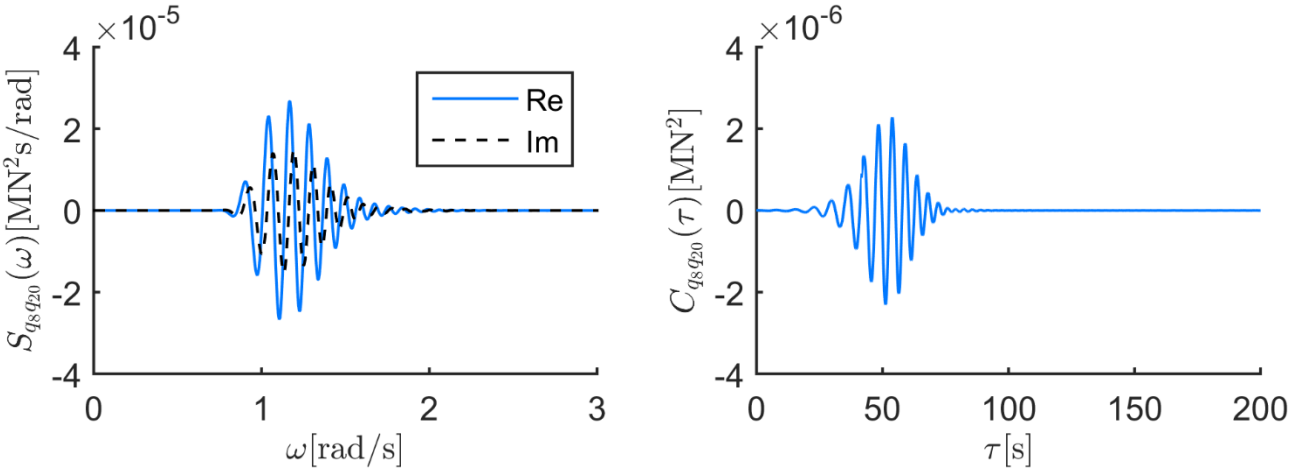

Figure 7. The cross-spectral density $S_{q_8q_{20}}(\omega)$ (left) between the loads in the sway directions of pontoon 2 and pontoon 4, along with the corresponding cross-covariance function $C_{q_8q_{20}}(\tau)$ (right).

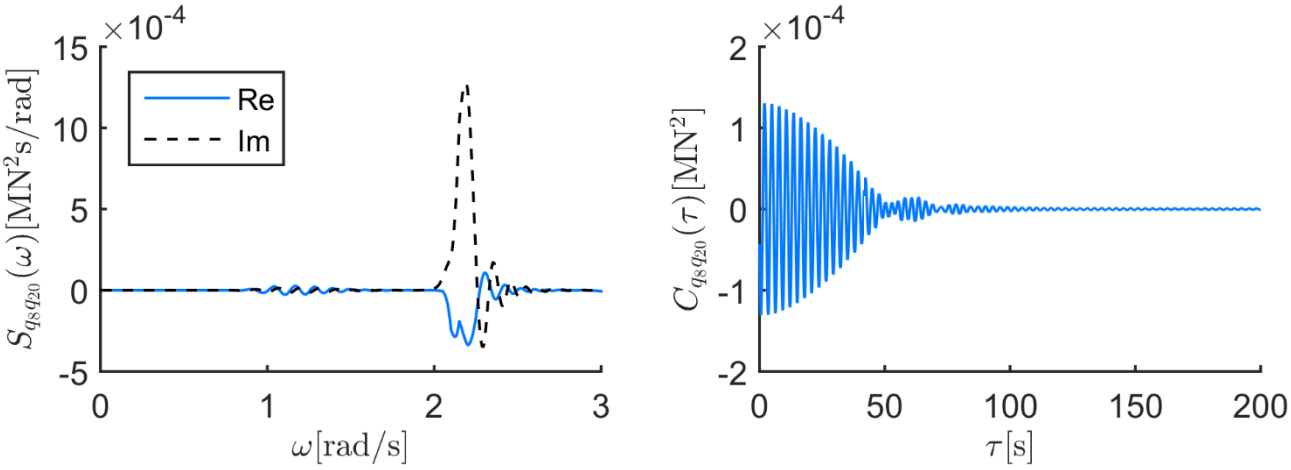

Figure 8. The cross-spectral density $S_{q_8q_{20}}(\omega)$ as calculated by using the trapezoidal rule with 100 integration points (left), along with the corresponding cross-covariance function (right).

5.2 Comparison of performance

Traditionally, the auto- and cross-spectral densities have been calculated by using the trapezoidal rule for numerical integration to solve the integral (6). This requires, however, great care with respect to the number of integration points that are used. The reason is that for large values of $\kappa(\omega)$ and large distances Δx or Δy, the complex exponential factor $e^{-i\kappa(\omega)(\Delta x \cos\theta + \Delta y \sin\theta)}$ will oscillate very fast with respect to the integration variable θ. This type of error is illustrated in Figure 8, where the cross-spectral density $S_{q_8 q_{20}}(\omega)$ is calculated using the trapezoidal rule with 100 integration points. When comparing with Figure 7, we see that large errors have been introduced for high frequencies, which in turn produce large errors for the cross-covariance. When using the series expansion method from Section 3, this problem is avoided.

The computation time for the calculations that must be repeated for different wave directions was recorded. When using the series expansion at 60 frequencies, the time was 0,7 seconds. In comparison, when using numerical integration, the time was 1,9 seconds. The methods were also compared for a chained floating bridge [9] with pontoon arrangement as shown in Figure 9. This bridge has a length of almost 5 kilometres and has 18 pontoons. In this case, the respective computation times were 5 seconds and 226 seconds, revealing that the series expansion method is superior when the length of the bridge is large.

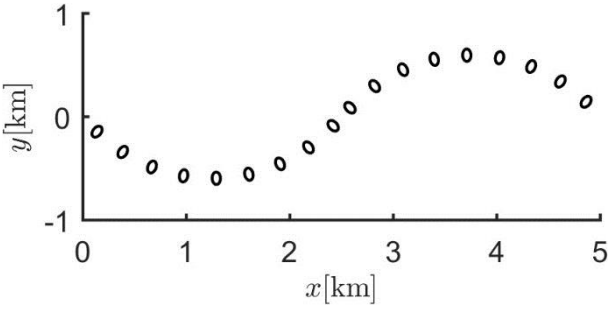

Figure 9. Pontoon locations and orientations for the chained floating bridge.

6 Conclusions

A fast and accurate approach for calculation of the auto- and cross-spectral densities has been presented. The approach has been illustrated for a pontoon type floating bridge, and the performance relative to the traditional method was investigated. The new approach appears to outperform the traditional approach, both in accuracy and computational effort. Furthermore, the gain in computational effort is seen to increase with increasing bridge length.

7 References

[1] Langen I., Sigbjörnsson R. On Stochastic Dynamics of Floating Bridges. *Engineering Structures*. 1980; **2**(4): 209-216.

[2] Kvåle K.A., Sigbjörnsson R., Øiseth O. Modelling the Stochastic Dynamic Behaviour of a Pontoon Bridge: A Case Study. *Computers and Structures*. 2016; **165**: 123-135.

[3] Sagrilo L., Næss A., Doria A. On the Long-term Response of Marine Structures. *Applied Ocean Research*. 2011; **33**(3): 208-214.

[4] Sigbjörnsson R. Stochastic Theory of Wave Loading Processes. *Engineering Structures*. 1979; **1**(2): 123-135.

[5] Hauser D., Kahma K., Krogstad H. *Measuring and Analysing the Directional Spectra of Ocean Waves*. Luxembourg: Publications Office of the European Union; 2005.

[6] Stansberg C.T., Contento G., Hong S.W., et al. The Specialist Committee on Waves Final Report and Recommendations to the 23rd ITTC. *Proceedings of the 23rd ITTC*. 2002; 505-736.

[7] DNV. *SESAM User Manual Wadam Wave Analysis by Diffraction and Morison Theory*. 2014.

[8] Ochi M.K. *Ocean Waves*. Cambridge: Cambridge University Press; 1998.

[9] Opgård B., Allievi F. Chained Floating Bridge. *IABSE Symposium Report*. 2014; **102**: 1236-1243.